HELICOPTER BLADE TWIST OPTIMIZATION IN FORWARD FLIGHT

Marco Lonoce, marcolonoce@libero.it, (Italy)

Filipe S.R.P. Cunha, filipescunha@tecnico.ulisboa.pt, IDMEC, LAETA, Instituto Superior Técnico (Portugal)

ABSTRACT

Improving the efficiency of the helicopter is one of the main objectives in helicopter design. Endurance, ceiling and maximum forward flight are strongly connected with the aerodynamic field around the main rotor and its power consumption, in particular the induced power used to generate the thrust needed to fly. It's possible to minimize this power with the uniformization of the inflow along the blade for all the azimuthal positions. The main objective of this paper is to find for each flight condition the blade twist distribution that minimizes power. The model is based on Blade Element Momentum theory for hovering condition and Blade Element theory for forward flight. It is tested using the flight test data of the UH-60A. The idea is to divide the blade in sections and impose on them a linear or quadratic twist behaviour. The first concept use only a section with linear or quadratic twist distribution. The second concept uses two segments each with a linear twist distribution. In this study different inner segments were analysed corresponding to 40%, 50%, 60% and 70% of the blade length. Finally, the last concept takes in account the main rotor of the Sikorsky UH-60A Black Hawk. It considers three sections and two airfoils and the twist behaviours are linear in each segment.

Nomenclature

A_{ed} Equivalent Wetted Area
B Coefficient for effective Blade Radius
C_l Coefficient of Lift
C_d Coefficient of Drag
D_{par} Parasitic Drag
f Tip or Hub loss parameter
F Correction Factor for tip or hub loss
f_{drag} Drag Parameter
k_x Cosinus component for linear inflow model
k_y Sinus component for linear inflow model
L Lift
N_b Number of blades
r Adimensional radius
R Maximum radius of the blade
U_T Velocity component parallel to the rotor
U_P Velocity component perpendicular to the rotor
V Forward Speed
y Coordinate along the blade
α Angle of Attack
β Flapping Angle
β_0 Coning Angle
β_{1c} Cosinus first harmonic flapping Angle
β_{1s} Sinus first harmonic flapping Angle
χ Skew Angle
λ Inflow
σ Solidity
μ Advanced Ratio
ϕ Inflow Angle
ρ Density
ψ Azimuth
θ Blade Twist
Ω Rotor Shaft Speed

1 INTRODUCTION

In comparison to the airplanes, helicopters have some limitations: a lower maximum forward speed, a lower service ceiling and a smaller range. Improving all of these characteristics is an important objective in helicopter design and this can be achieved by an effective reduction of power consumption. The helicopter power consumption is essentially divided in four parts: main rotor induced power, main rotor profile power, fuselage parasitic power and tail power [1]. All of these aspects are strongly connected with the aerodynamic of the helicopter that, unfortunately, depends on the flight conditions. The purpose of this paper is to investigate the main rotor power reduction. There are several ways to do it and almost all of these are based on main rotor morphing [2]. Some examples are: variable rotor speed or diameter, active blade twist, trailing edge flaps or actuation system [3–6]. The study presented here analyses the blade twist morphing. According to the wind tunnel tests [7, 8], in hovering condition the helicopter needs high twisted rotor trying to have an inflow as uniform as possible. But on the other side, in forward flight condition it's possible to re-

duce the induced power with a rotor with a lower twist. Said that, it's important to understand which twist minimizes the induced power for each flight condition and then, to use those values with an Active Twist Control (ATC) [9].

The original idea of ATC system was utilized to reduce the vibration of the main rotor. In the 1990s there were some wind tunnel tests of smart rotors with an individual blade twist control, a piezoceramic material actuator [7, 8]. They understood that was possible to control with an "induced-strain actuation" the blade twist. In these experiments the target value was 1° or 2° to obtain reduction of vibrations. Now, the idea is to use a more powerful ATC system able to change all the twist distribution along the blade to have a main rotor optimized for all the flight conditions. The tests are done with an empirical/analytical method based on Blade Element theory (BET) and Blade Element Momentum theory (BEMT): the results have some limitations but in a first approximation it's possible to obtain good results with a small cost in term of computational time.

2 NUMERICAL MODEL

To analyse the aerodynamic characteristics of the helicopter a model based on BEMT and BET are used. The characteristics of the airfoils are taken from the software XFoil, a 2D simulation code based on panel method developed by Mark Drela in MIT [10]. The two main important, for this kind of analysis, are the coefficients of lift C_l and drag C_d that are function of the angle of attack α:

$$C_l = f(\alpha) \qquad C_d = g(\alpha) \tag{1}$$

The results don't represent continuous functions, they are given for several angles α of attack with $\Delta\alpha$ = 0.25 $^\circ$ as step. To implement an optimization code the input data have to be continuous so an interpolation is required. The database is interpolated using polynomial equations and the order is chosen to achieve the best fitting possible. In general simple models use a linear equation to represent lift curve and a quadratic one for the drag curve. High order polynomial equation can also represent stall condition and drag bucket to take in account all the airfoil informations. After that, the aerodynamic data are used to estimate the lift, the profile drag and the induced power of the main rotor. To describe hovering and forward flight conditions two models are taken in account. In hover [1], using the equivalence between the circulation and momentum theories of lift, allows the estimation of the inflow distribution along the blade. Considering no climb velocity the simplify model is [1]:

$$\lambda = \frac{\sigma C_{l\alpha}}{16F}\left(\sqrt{1+\frac{32F}{\sigma C_{l\alpha}}\theta r}-1\right) \tag{2}$$

Where λ is the inflow, σ the solidity, Cl_α the slope of the lift -α curve, θ the twist, r the radius and F the the correction factor for tip and hub loss.

Using this model, it's possible to estimate the inflow in function of the twist distribution. In forward flight, the helicopter must provide a lifting force and a propulsive force in opposition of weight and airframe drag. The rotor moves through the air and all the blade sections encounter a periodic variation in local velocity. There are some consequences as blade flapping, unsteady effects, non-linear aerodynamics, stall, reverse flow and an higher interference between rotor wake and the main rotor itself [1]. The induced velocity field is no longer axisymmetric and the effects of the individual tip vortices tend to produce a highly non-uniform inflow over the rotor disk specially during the transition from hover into forward flight, within the range: $0.0 \leq \mu \leq 0.1$ where $\mu = \frac{V}{\Omega R}$.
In higher speed forward flight (advanced ratio higher than 0.15) the time averaged longitudinal inflow becomes more linear and can be approximately by [1]:

$$\lambda_i = \lambda_0(1 + k_x r\cos\psi + k_y r\sin\psi) \tag{3}$$

The estimated values of first harmonic inflow considered in this paper is that one from Pitt and Peters (1981) [11, 12] that has a good representation of the inflow gradient as functions of the wake skew angle and the advanced ratio when compared to the experimental data.

$$k_x = \frac{15\pi}{23}\tan\frac{\chi}{2} \qquad k_y = 0 \tag{4}$$

The BET assumes that the blade can be divided into small elements that operate aerodynamically as 2D airfoils and the aerodynamic forces can be calculated considering just the local flow conditions. Due to the simplicity of the theory the assumption that the airflow field around the airfoil is always in equilibrium is necessary. There are also some corrections to account hub loss [13], tip loss [1] and reverse flow [1]. The only corrections that are not considered are the compressibility effects in high speed forward flight that increase the drag. For the hub and tip loss two corrections are considered, because BEM theory permits a finite lift to be produced at the blade tip that it's unrealistic. A factor B [13] of around 0.95 for the hub losses relation while for the tip loss the Prandtl tip-loss function it's considered. The latter considers a solution to

the problem of the loss of lift near the tips taking in account the induced effects related with a finite number of blades. The two relations for hub and tip are pretty similar [1, 13]:

$$(5) \qquad f_{tip} = \frac{N_b}{2}\frac{1-r}{r\phi} \qquad \text{and} \qquad f_{hub} = \frac{B}{2}\frac{r-r_{min}}{r\phi}$$

and the correction factor F [1, 13], that modifies the coefficient of lift C_l along the blade, is calculated for each situation as:

$$(6) \qquad F_{tip} = \frac{2}{\pi}\arccos(e^{-f_{tip}}) \qquad \text{and} \qquad F_{hub} = \frac{2}{\pi}\arccos(e^{-f_{hub}})$$

Another contribution to take in account is the Parasitic Drag that is important to understand how the coefficient of thrust has to change to compensate not only the weight but also the drag of the helicopter. The model used is [1]:

$$(7) \qquad D_{par} = \frac{1}{2}\rho V^2 f_{drag} A_{eq}$$

where the drag parameter f_{drag} and the equivalent wetted area A_{eq} are related with the helicopter type.

This work also takes in account the blade flapping [1]. The hinge offset is neglected to simplify the calculation and the second order differential equation is:

$$(8) \qquad \overset{**}{\beta} + \beta = \frac{1}{I_b\Omega^2}\int_0^R Ly dy \qquad \beta = \beta(\psi)$$

where for definition the flapping β is function of the azimuthal position ψ,$\beta = \beta(\psi)$. To solve the differential equation the first harmonic of the movement is imposed:

$$(9) \qquad \beta(\psi) = \beta_0 + \beta_{1c}\cos\psi + \beta_{1s}\sin\psi$$

Now, to compute the thrust and power of the main rotor the components of the velocity parallel to the blade leading edge U_T and perpendicular to the rotor U_P have to be considered:

$$(10) \qquad \begin{aligned} U_T(y,\psi) &= \Omega y + \mu\Omega R\sin\psi \\ U_P(y,\psi) &= \lambda_i\Omega R + y\dot{\beta}(\psi) + \mu\Omega R\beta(\psi)\cos\psi \end{aligned}$$

Where y is the radial coordinate, Ω the rotor shaft speed and R the maximum radius of the blade. The angle of attack α can be expressed in function of the twist angle θ and the inflow angle ϕ :

$$(11) \qquad \alpha = \theta - \phi \qquad \text{and} \qquad \phi = \arctan(\frac{U_P}{U_T})$$

The BET [1] gives for the incremental lift dL and drag dD:

$$(12) \qquad dL = \frac{1}{2}\rho U^2 c C_l dy \qquad \text{and} \qquad dD = \frac{1}{2}\rho U^2 c C_d dy$$

where c is the chord, $C_l = f(\alpha) = f_2(y,\psi)$ and $C_d = g(\alpha) = g_2(y,\psi)$. So the equations of thrust T and power P can be written as:

$$(13) \qquad \begin{aligned} T &= \iint N_b dF_z = \iint N_b(dL\cos\phi - dD\sin\phi) \\ P &= \iint N_b dF_x \Omega y = \iint N_b(dL\sin\phi + dD\cos\phi)\Omega y \end{aligned}$$

where dF_x the force parallel to the rotor disk while dF_z the force perpendicular. Replacing equations 12 and 10 inside thrust and power equations 13 in a general form the two forces, parallel and perpendicular to the rotor disk, can be expressed as two functions of azimuth and radial position:

$$(14) \qquad dF_z = \mathcal{F}_z(y,\psi)dydy\psi \qquad \text{and} \qquad dF_x = \mathcal{F}_x(y,\psi)dydy\psi$$

$$(15) \qquad \begin{aligned} T &= \frac{1}{2\pi}\int_{R_{min}}^{R_{max}}\int_0^{2\pi} N_b\mathcal{F}_z(y,\psi)dyd\psi \\ P &= \frac{1}{2\pi}\int_{R_{min}}^{R_{max}}\int_0^{2\pi} N_b\Omega y\mathcal{F}_x(y,\psi)dyd\psi \end{aligned}$$

The code is implemented in Matlab and it's able to compute the twist distribution that minimizes power ([**?**]) for each flight condition. Matlab 'Fmincon' [14] function is used for the optimization process combined with a global search [15] for the minimum. This function can calculate a local minimum given initial conditions while the global search creates a system of different initial conditions to obtain all the minimum solutions and after it will take the global one.

To obtain the flapping solution [1] an ordinary differential equation solver from Matlab, 'ode45', is used. This solver is based on Runge-Kutta methods, a family of implicit and explicit iterative methods used in temporal discretization for the approximate solutions of ODE [16].

3 COMPARISON WITH FLIGHT DATA

To validate the method the flight data of the UH-60A helicopter is used [17–20]. To make a comparison between simulations and flight data all the typologies of power have to be taken in account. The code calculates the main rotor induced power, main rotor profile power and fuselage parasitic power. The tail rotor power is estimated as 5% more the power consumption of the helicopter. The distance between the hub centre of the tail rotor and the rotor shaft in the UH-60A is 9.926 m. In all the calculations the weight of the helicopter is W = 8322.4 kg [21].

Table 1. UH-60A Data [21]

Main Rotor Parameters	
Main Rotor Radius	8.1788 m
Nom. Main Rotor Speed	27.0 rad/s
Blade Chord Lenght	0.5273 m
Blade Twist	Nonlinear
Blade Airfoil	SC1095/SC1094R8
Number of Blades	4
Blade Mass/length	13.92 kg/m

The blade twist of the UH-60A is non linear and presents some transition areas for the presence of different airfoils. To simplify the calculation that behaviour is approximated by a linear blade twist of -16° and only the SC 1095 airfoil.

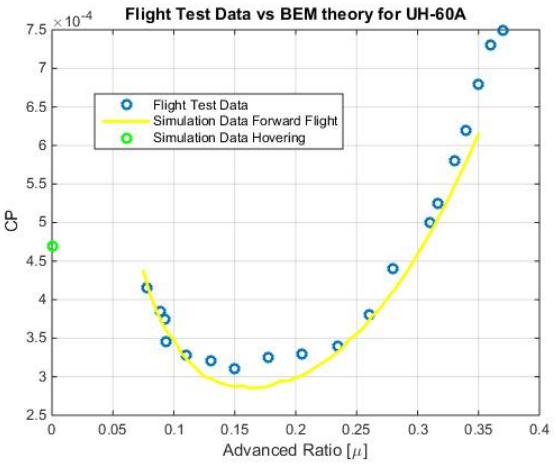

Fig. 1. Comparison between Flight Test Data and Simulation with BET and BEMT for UH-60A

Fig. 1 shows the comparison between flight test and the results from the method. Due to the limitation related to the linear model applied in low advanced ratio range, the calculations are done for advanced ratio higher than 0.075. The predictions, using a simple model, are in good agreements with the flight test data and for that reason the application of this method in the analysis of the helicopter performance is verified.

4 EFFECT OF BLADE TWIST ON MAIN ROTOR POWER

High twisted blades improve hover, vertical climb and low speed performance, for example, for military helicopters nap-of-the-earth performance capability [22,23]. From the aerodynamic point of view in hovering condition, the result is a more uniform downwash velocity in the far wake that corresponds to a reduction of induced power required [22]. In 1987 Keys et al. [22] conducted a test to quantify the effect of twist on performance and aicraft vibrations. They considered a four bladed rotor with Mach scaled composite blades and they tested it in a wind tunnel with two linear twist distributions: -11.5° and -17.3°. Increasing the blade twist, in hovering condition, showed a reduction of 2.4% on power required that corresponds in a 5% increase in useful load [22]. The experiment also showed that the new redistributed downwash velocity in the inboard part of the rotor increased the aerodynamic load on the fuselage of 6%. So, the benefit of the twist was reduced of 15% [22].

According to the theory [1], in hovering situation an hyperbolic variation of twist $\frac{\theta_0}{y}$ has the minimum induced power. This solution is not physically possible because it's not feasible to build a blade with this shape (the angle near the root would be too big). Nevertheless a linear twist distribution can improve the performance is a similar way as the hyperbolic twist variation.

The characteristics of UH-60A Sikorsky in table 1 are used to show the effect of blade twist using BEM theory for hovering condition and BET for forward flight. There are some differences from the real helicopter: in this analysis only the SC 1095 airfoil is considered and the twist distribution is linear. In fact the comparison is among 6 blade twist behaviours: no twist, -4° linear twist, -8° linear twist, -12° linear twist, -13.5° linear twist, -16° linear twist. The condition with -13.5° linear twist is considered only in hovering situation.

In Fig. 2 is showed the effect of different twist distributions in hovering condition. In this example the coefficient of power decreases if the linear twist slope is increased. This is not true for the simulation with -16° because the inner part of the blade stalls. The effect is a reduction of the lift and a increase of drag. Using the optimization procedure the optimum linear twist for a hovering condition and the single profile was found to

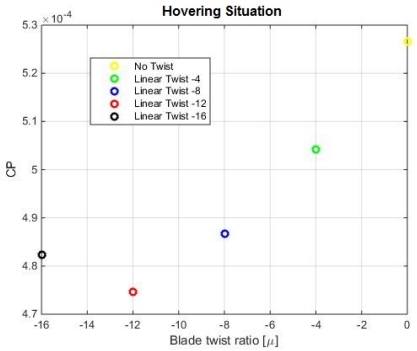

Fig. 2. Total power for different linear twist distributions in Hovering

be -13.5°. So a solution with -16° presents higher twist slope than the optimal one. This solutions came from an analysis with BEM theory with tip and hub losses and airfoil characteristics from the simulation of Xfoil. Also, the reduction of the benefit of the download [22] is not considered.

In forward flight the effect of blade twist is different. In 1948 there was a study [24] that indicated that higher blade twist reduced forward flight power based on flight test data. This conclusion looks strange at present time but in that period the early helicopters were limited to 130km/h, in low speed forward flight highly twist blades are able to reduce the coefficient of power as shown in Fig. 3.

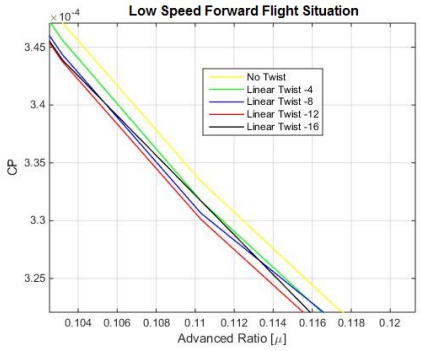

Fig. 3. Total power for different linear twist distributions in low speed forward flight

Modern helicopters can easily reach a speed of 300km/h. The required blade twist distribution to minimize the power consumption slowly decreases if the forward flight increases. The results are showed in Fig. 4 and Fig. 5.

In Fig. 4 it's evident that after $\mu = 0.18$ the linear twist distribution with $-8°$ of slope becomes the solution that requires less power. Finally, in Fig. 5, in high speed forward flight a linear twist behaviour of $-4°$ presents better results.

Keys et all in 1987 [22] studied the four bladed rotor with Mach scaled composite blades also in forward

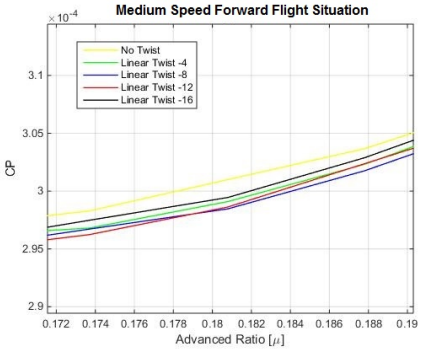

Fig. 4. Total power for different linear twist distributions in medium speed forward flight

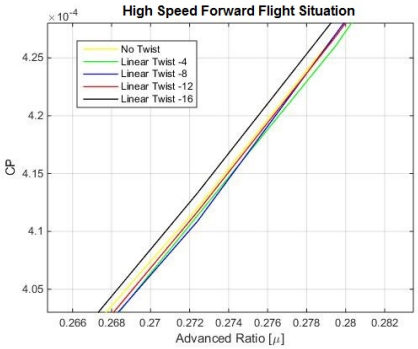

Fig. 5. Total power for different linear twist distributions in high speed forward flight

flight with the two linear twist distributions of $-11.5°$ and $-17.3°$. The solution with high twisted blade presented a measured power increment of 5% at 330km/h. They also calculated that the helicopter with $-17.3°$ linear twist distribution presented the same power consumption of the $-11.5°$ at 330km/h around 322.5km/h. So the performance penalty due to twist was approximately 7.5km/h.

5 OPTIMIZED BLADE TWIST

An optimal blade twist behaviour, in function of the forward flight, is determined by what kind of twist is imposed. Some examples use a linear twist, others a non-linear blade twist, and for cases of a blade with more than one airfoil each blade section could have a different blade twist. The more complex is the function that describes that the blade twist more advantages are possible to achieve in term of power reduction. According to recent studies [25], three sections blade is a solution to take in account the different aerodynamic environments along the blade for each flight condition. For example in the British Experimental Rotor Program (BERP) [25] the blade is divided in three sections with three different airfoils. The central section has the main lifting airfoil, the RAE 9645, has a maximum lift coefficient of about 1.55. However, this

high lift coefficient is obtained at the expense of higher pithing moments that is counterbalanced by the airfoil in the inner part, the RAE 9648, where the high maximum lift is not so important. In the tip the airfoil is the RAE 9643 that is a low thickness-to-chord ratio to increase the divergence Mach number. This is really important to increase the maximum speed of the helicopter. So, a solution with three different segments is commonly used and for each section, there is a particular airfoil that needs a different twist behaviour for the optimization.

In the simulations, for each flight condition between hovering condition and high speed forward flight with $\mu = 0.35$ the twist slope that minimizes the power consumption is found. Another main aspect is the accuracy of the model developed to simulate the helicopter, it is based on BEM and blade element theory and cannot achieve the accuracy of models based on free vortex methods. ElQatary et all [27], did a comparison between CFD and BEMT models. The differences in power consumption were in a range between 2.2% and 7%, so the error has an order of kWatt. Now, considering a flight condition, for example $\mu = 0.2$, and two solutions really close one to the other, with just a small difference in the twist distribution, the difference in power consumption has an order of Watt or at least hundreds of Watt. So, the power consumption will be really close and this will not affect the comparison with the flight data and the validity of the code but the accuracy it's not enough to determine which solution minimizes the power consumption. So, the results shown present some fluctuations and it's necessary to interpolate the simulations to obtain the twist behaviours.

5.1 One section with linear twist

The first analysis considers a rectangular blade with only the SC 1095 Airfoil. The blade twist distribution is linear from the root until the tip. Fig. 6 shows how the twist slope should change to minimize the power consumption.

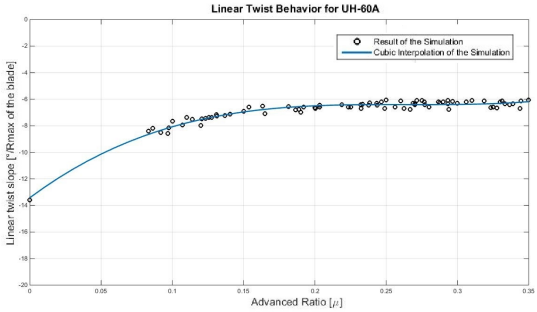

Fig. 6. Optimum linear twist slope for each advanced ratio μ for UH-60A

The hovering condition requires $-13.5°$ of twist slope along the blade. The required slope decreases really fast around $\mu = 0.1$ the required slope is around $-8°$. Around $\mu = 0.2$ the twist slope reaches $-6°$ and it increases really slowly with the advanced ratio.

5.2 Quadratic Twist

A quadratic twist behaviour along the blade with just one segment is also considered. The twist follows a parabolic equation. There are three possible applications: the first one considers the minimum of the parabola exactly in the tip of the blade and the others a minimum inside the blade or without a minimum. To simplify the calculation the minimum is considered at the end of the blade.

$$\theta = ar^2 + br + c \tag{16}$$

Where θ is the twist, r the adimensional radius, a,b,c the three coefficients that characterize the shape of the parabola.
Imposing the first derivative equal to zero in the tip:

$$\frac{d\theta(r=1)}{dr} = 2a + b = 0 \qquad b = -2a \tag{17}$$

Considering a minimum exactly in the tip reduces the number of variables. So, it's possible to study a non-linear twist distribution without increasing the computational time to obtain the results.
In Fig. 7 the change of this parameter with forward speed is shown.

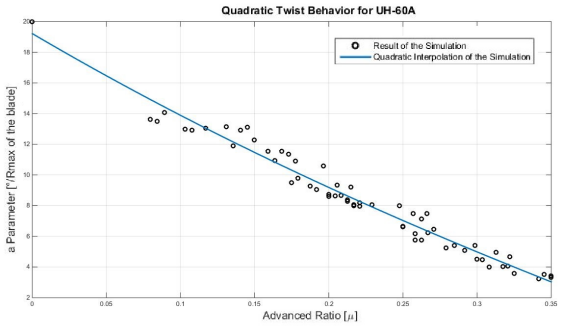

Fig. 7. a parameter of the parabolic equation - Optimum quadratic twist in function of advanced ratio μ for UH-60A

Fig. 8 shows the difference of the twist between root and tip for the quadratic twist distribution. In hovering the value is around $7°$ and in high speed forward

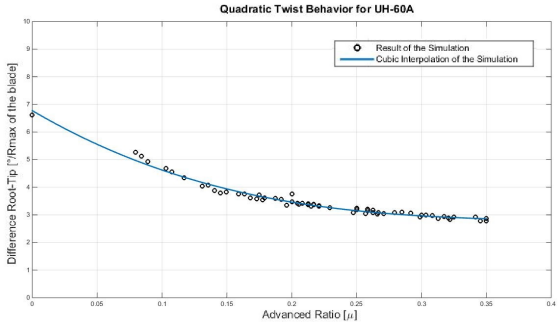

Fig. 8. Difference tip and root twist - Optimum quadratic twist in function of advanced ratio μ for UH-60A

flight is less than $3°$. So, the active twist control concept for the quadratic twist has to reduce the difference from root and tip only of $4°$. Doing a comparison with the concept with one section and linear twist it requires $-13.5°$ of twist slope in hovering condition that has to be reduced to $-6°$ increasing the forward flight. So, the active twist control has to reduce the twist slope of $7.5°$. Fig. 7 shows how the a parameter changes with forward speed. This coefficient characterizes the shape of the parabola, in hovering is around of 20, so the twist has to change really fast increasing a little bit the forward speed.

5.3 Two sections with linear twists

In the following condition two linearly twisted segments are considered. In a situation like this one, there is an extra parameter that is how to divide the blade in two segments. In order to understand the effects of the different division four conditions are presented: 40%, 50%, 60% and 70% of the blade length for the inner part.

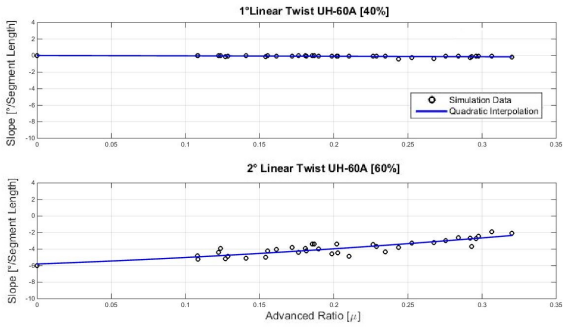

Fig. 9. Optimum two linear twist slopes in function of advanced ratio μ for UH-60A. Blade division in 40% - 60%

Fig. 9 considers a division in 40% for the inner part and 60% for the outer part. Increasing the forward flight in this condition weakly affects the inner part that looks almost constant and the outer has the theoretical behaviour where the twisted ratio is reduced in high speed forward flight condition. For the hovering condition was not possible to find the minimum using the optimization code due to the strongly non-linear equation that describes the inflow along the blade (when the optimization code, during the iteration, gets complex numbers fails). For this reason and due to the fact that all the simulations in forward flight present almost constant twist, the hovering condition is calculated fixing the inner part of the blade to the value of the forward flight and optimizing only the outer part. This solution couldn't represent the minimum power consumption in hovering but gives advantages in term of active twist control implementation.

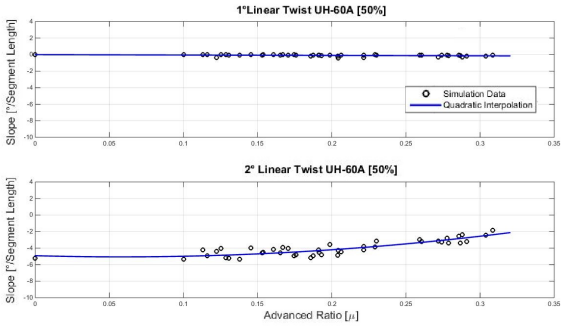

Fig. 10. Optimum two linear twist slopes in function of advanced ratio μ for UH-60A. Blade division in 50% - 50%

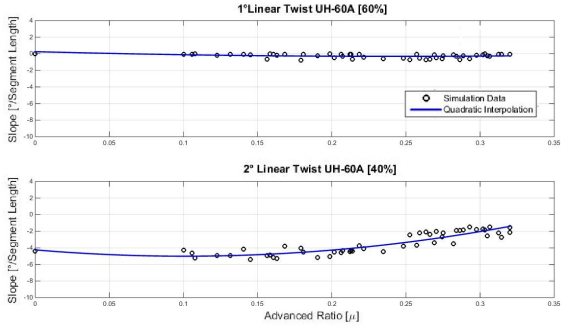

Fig. 11. Optimum two linear twist slopes in function of advanced ratio μ for UH-60A. Blade division in 60% - 40%

All of these simulations present higher oscillations that the other behaviours taken in account due to the increase of one variable in the optimization code (root and tip twist angle for the one segment linear twist and 'c' and 'a' parameters in the non-linear twist ratio). Fig. 10 divides the blade exactly in half. Also here it's possible to assume only one linear twist for all the flight conditions in the first segment. Fig. 11 is the opposite of the first graph and the approximation looks feasible

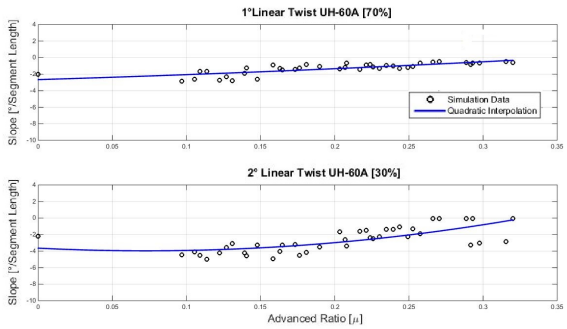

Fig. 12. Optimum two linear twist slopes in function of advanced ratio μ for UH-60A. Blade division in 70% - 30%

yet. Fig. 12 considers 70% of the blade for the inner part and just 30% for the outer part. The inner part has a different behaviour and it's not possible to consider only one linear twist for all the flight conditions.

5.4 Two sections with linear twist and different airfoils

All of these simulations consider only the SC 1095 airfoil, in the next picture the blade it's exactly divided in two egual parts but two airfoils, the SC 1095 and the SC 1094R8 are used:

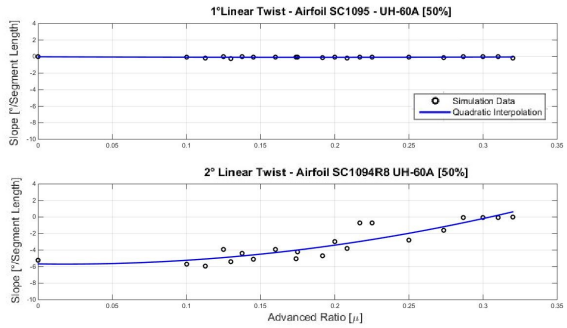

Fig. 13. Optimum two linear twist slope in function of advanced ratio μ for UH-60A. Two airfoils SC 1095 and SC 1094R8 with blade division 50% - 50%

Also here, the hovering condition is calculated fixing the inner part to the forward flight value and just optimizes the outer part twist slope.
The results are quite interesting for the engineering point of view. Thinking about an implementation on a real rotor could be possible to fix the inner part of the blade and introduce an active twist control only in the outer part. This kind of solution could reduce the power consumption of the helicopter without introducing too much weight and other complex elements inside the blade. The concepts with linear or quadratic distributions require an active twist system that has to modify the twist behaviour from the root to the tip of the blade. According to some studies [9, 28], a possible solution is to use piezoelectric actuators that have to be spread along the blade. Each one required a certain amount of power to generate the electric field to use the actuators. But, these concepts with two segments present an inner part of the blade that doesn't require a new redistribution of the twist and for this reason it's necessary to place the actuators only in the outer part. The system requires less actuators that means less electrical power and less weight.

5.5 Three linear segments

The last behaviour is directly related to the blade shape of the UH-60A: the idea is to consider three different sections with linear twist with two different airfoils. The real helicopter has a non-linear twist behaviour divided in three sections but in this analysis three linear segments are considered. In the following picture [20] the blade shape of the UH-60A Sirkosky is presented.

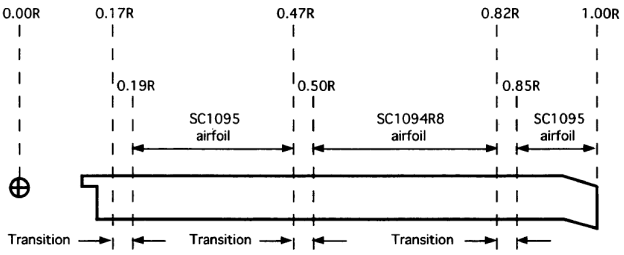

Fig. 14. Blade planform and shape of UH-60A [17]

To simplify the model all the transitions areas are not considered and also the final taper is neglecting. The tip shape is related to compressibility effects that in this model are not considered. The new division is the first half of the blade for the first segment, the second another 35% of the blade and the third just the last 15%.

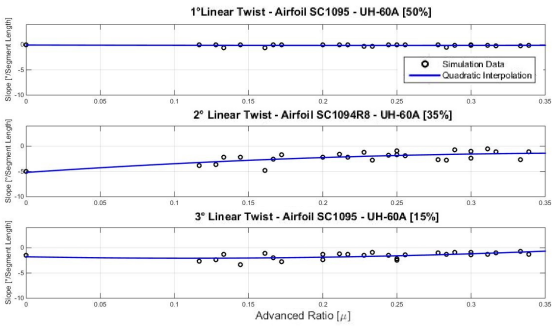

Fig. 15. Optimum 3 linear twist slopes in function advanced ratio μ for UH-60A

The solution shows a behaviour similar to the two linear segments, the inner part presents a constant twist for all the flight conditions. The hovering condition is calculated fixing the inner and outer part with the same values of the forward flight that are almost constant for the reasons presented before. The outer part has also constant twist but the central segment shows a twist behaviour that decreases the slope increasing the forward speed. This simulation presents, as the other, some oscillations in the results, the complexity of the model in this condition is related with four parameters that have to be optimized and these are the tip, the root and the two nodes that connected the three linear segments. Increasing the forward flight all the results have less wiggling because the inflow model used describes in a better way the reality with high speed forward flight. Thinking about an engineering application of this solution is necessary to implement an active twist control just for the second part of the blade and it's possible to fix inner and outer parts.

6 COMPARISON AMONG THE SIMULATIONS

Table 2. Reduction of power between Fixed linear twist slope of -13.5° and simulations

Simulation concept	Power Reduc.
Linear twist	-1.34%
Quadratic twist	-8.65%
2 Seg. with 40% - 60%	-4.86%
2 Seg. with 50% - 50%	-4.46%
2 Seg. with 60% - 40%	-3.44%
2 Seg. with 70% - 30%	-2.55%
2 Seg., 2 airf. 50% - 50%	-2.21%
3 Seg., 2 airf. 50% - 35% - 15%	-6.09%

Table 2, presents a comparison among all the simulation concepts with a fixed linear twist distribution of -13.5° that is the value of twist slope that optimizes the hovering condition of a rotor with only the SC 1095 airfoil and linear twist distribution along the blade.
Using a linear twist with active twist control can reduce the power consumption of 1.34%. The other solutions give better results, in fact the concepts with two segments can reach a reduction of 4.46%. All of these concepts fix the inner part twist and use an active twist control only for the outer part. The two segments with 40% - 60% blade division can get higher performance in comparison to the others because the controlled part is higher (the 60%). At the end there are two concepts: quadratic twist behaviour and three segments with linear twist that are the two best conditions with 8.65% and 6.09% of power consumption reduction.
In Fig. 16 linear twist, quadratic twist and three linear twist segments are plotted.

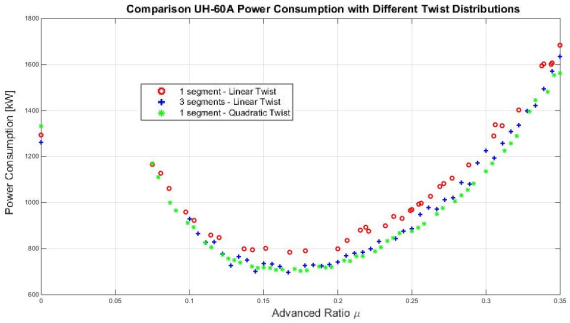

Fig. 16. Power consumption in function of advanced ratio μ for different twist behaviours.

The simulations show, for each flight condition, the power consumption of the UH-60A in function of the advanced ratio μ. The blade twist, needed to minimize the power consumption, changes according to the behaviours calculated in the previous section.
Fig. 16 represents a graphic point of view of the power reduction achievable with the different concepts. Already is known that the linear twist distribution gives the lowest benefit while the other conditions the highest. Looking only to the hovering the three linear twist segments concept gives the lower power consumption but after $\mu = 0.25$ the quadratic twist distribution has better values. For this reason, in term of power consumption reduction the non-linear twist represents the best condition.

From an engineering point of view, centred on a possible application with active twist control, there are some other aspects that have to be taken in account. The non-linear concept requires an active twist control that involves all the blade from the root to the tip while the three linear twist segments can just use a system for the second segment for only 35% of the blade. In the non-linear concept the twist morphing requires higher variations of the parameters that could produce problems related to fatigue and deformations. Also the weight, the power consumption and the forces required of the actuator in the three linear twist segments are lower because the system has to control only the 35% of the blade.
After these considerations, looks easier to implement an active twist control for the three linear twist sections than for the non-linear twist distribution.

7 CONCLUSIONS

In this paper variable blade twist is used to reduce rotor power and improve helicopter performance. Simplified models based on BEM theory for hovering condition and BET for forward flight to calculate the aerodynamics loads of the helicopter are used [1]. The database of the airfoils is obtained by a simulation using Xfoil for 2D profile. The inflow models are analytical, one for hovering condition [1] and the other Pitt - Peters model [11,26] that gives higher correlation with flight data for advanced ratio higher than 0.1. All the effects due of tip and hub loss, reverse flow and flapping behaviour are also considered [1, 13]. Several solutions are taken into account and all of those can reduce the power consumption and optimize the helicopter in each flight condition: one section with linear or quadratic twist behaviour, two sections with linear twist distributions but different blade divisions with one or two airfoils and finally the three sections linearly twisted with two airfoils. The best solution comes from a compromise between complexity, weight and power consumption of the active twist control system and benefit produced by the actuation. In term of power consumption reduction a comparison among all the concepts is done. The reference condition is a fixed linear twist distribution of -13.5° of slope. The highest power consumption reduction comes from the simulation with one section and quadratic twist distribution and the result is 8.65%. The concept with linear twist along one section gives the lowest power consumption reduction around 1.34%. Another concept with good result is the three linear sections that can provide a power consumption reduction around 6.09%. All the concepts with two or three sections show something interesting, the twist slope of the inner part of the blade remains almost constant changing the advanced ratio and in the three sections concept also the outer part remains almost with constant slope. So they don't require an active twist control system that has to be spread along all the blade. Taking in account the main interesting concepts, the three sections and the quadratic there are some differences: the non-linear concept requires an active twist control that involves all the blade from the root to the tip while for the three linear sections it's enough to placed the ATC in the central section for just 35% of the blade length. So, there are advantages about electrical power consumption and reduction of the weight of the actuators.

8 ACKNOWLEDGMENTS

This work was supported by FCT, through IDMEC, under LAETA, project UIDB/50022/2019.

References

[1] Leishman, J. G., 2006. *Principles of Helicopter Aerodynamics*, 2^{nd} ed. Cambridge Aerospace Series. ISBN:9780521523967.

[2] A., P., and S., A., 2011. "Helicopter Blade Morphing Strategies Aimed At Mitigating Environmental Impact ". *Journal of Theoretical And Applied Mechanics,* **49**(4), pp. 1233–1259.

[3] Paternoster, A., 2013. "Smart Actuation Mechanisms for Helicopter Blades". PhD thesis, University of Twente, Enschede, The Netherlands, Febraury.

[4] Koratkar, N., and Chopra, I., 2001. "Wind Tunnel Testing of A Mach-Scaled Rotor Model with Trailing-edge Flaps". *Smart Materials and Structures,* **10**(1), p. 1.

[5] Viswamurthy, S., and Ganguli, R., 2004. "An Optimization Approach to Vibration Redution in Helicopter Rotors with Multiple Active Trailing Edge Flaps". *Aerospace Science and Technology,* **8**(3), pp. 185–194.

[6] Wilbur, M., Mirick, P., Yeager, W., Langston, C., Cesnik, C., and Shin, S., 2002. "Vibratory Loads Reduction Testing of the NASA/Army/MIT Active Twist Rotor". *Journal of the American Helicopter Society,* **47**(2), pp. 123–133.

[7] Chen, P., and Chopra, I., 1997. "Numerical Optimization of Helicopter Rotor with Induced-Strain Actuation of Blade Twist". *AIAA Journal,* **35**(1), pp. 6–16.

[8] Chen, P., and Chopra, I., 1997. "Wind Tunnel Test of a Smart Rotor Model with Individual Twist Control". *Journal of Intelligent Material Systems and Structures,* **8**(5), pp. 414–425.

[9] Kovalovs, A., Barkanov, E., and Gluhihs, S., 2007. "Numerical Optimization of Helicopter Rotor Blade Design for Active Twist Control". *Institute of Materials and Structures, Riga Technical University,* **11**(3), pp. 3–9.

[10] Drela, M., 2013. "Xfoil Software and Documentation". *Xfoil 6.99 (Unix, Windows)*, p. http://web.mit.edu/drela/Public/web/xfoil/.

[11] Chen, R., 1989. "A Survey of Non-uniform Inflow Models for Rotorcraft Flight Dynamics and Control Applications". *NASA Technical Memorandum 102219*, pp. 64–3 – 64–20.

[12] Peter, A., Doug, D., and Cheng, H., 1989. "Finite - State Induced Flow Model for Rotors in Hover and Forward Flight". *Journal of American Helicopter Society,* **34**(4), pp. 5–17.

[13] Moriarty, P., and Hansen, A., 2005. "Aerodyn Theory Manual". *Natiojnal Renewable Energy Laboratory*.

[14] Mathworks, F. M., 2016. "Find Minimum of Constrained Non-linear Multivariable Function". *http://it.mathworks.com/help/optim/ug/fmincon.html*.

[15] Mathworks, G. S. M., 2016. "Find global minimum". *http://it.mathworks.com/help/gads/globalsearch-class.html*.

[16] ODE45, M. M., 2016. “Solve Nonstiff Differential Equation”. *http://it.mathworks.com/help/matlab/ref/ode45.html*.
[17] Totah, J., 1993. “A Critical Assessment of UH-60 Main Rotor Blade Airfoil Data”. *Technical Report NASA - 103985*.
[18] Yeo, H., Bousman, W., and Johnson, W., 2004. “Performance Analysis of a Utility helicopter with Standards and Advanced Rotors”. *Journal of American Helicopter Society,* **49**(3), pp. 250–270.
[19] Davis, S., 1981. “Predesign Study for a Modern 4-bladed Rotor for the RSRA”. *Technical Report NASA - CR - 166155*.
[20] Bousman, W., 2003. “Aerodynamic Characteristics of SC1095 and SC1094 R8 Airfoils”. *NASA / TP - 2003 - 212265*.
[21] Han, D., Pastrikakis, V., and Barakos, G., 2016. “Helicopter Performance Improvement by Variable Rotor Speed and Variable Blade Twist”. *Aerospace Science and Technology,* **54**, pp. 164–173.
[22] Keys, C., and Tarzanin, F., 1987. “Effect of Twist on Helicopter Performance and Vibratory Loads”. *13th European Rotorcraft Forum*.
[23] Paul, W., and Zincone, R., 1977. “Advanced Technology Applied to the UH-60A and S-76 Helicopters”. *3rd European Rotorcraft and Powered Lift Forum*.
[24] Gessow, A., and Myers, G., Republished in 1967. *Aerodynamics of the Helicopter*. Frederick Ungar Publishing Co.
[25] Perry, F., WIlby, J., P., and Jones, G., 1998. “The BERP Rotor - How Does it Work and What Has it Been Doing Lately?”. *Vertuffute,* **44**(2), pp. 44–48.
[26] Pitt, D., and Peters, D., 1981. “Theoretical Prediction of Dynamic Inflow Derivatives”. *Vertica,* **5**, pp. 21–34.
[27] ElQatary, I., and Elhadidi, B., 2014. “Comparison between OpenFOAM CFD and BEM theory for Variable Speed and variable pitch HAWT”. *ITM Web of Conferences 2*.
[28] Wilbur, M., and Wilkie, W., 2004. “Active Twist Rotor Control Applications for UAVs”. *Proceeding of the 24th Army Science Concerefence,* **42**, p. 185.